ORCA – Online Research @ Cardiff

This is an Open Access document downloaded from ORCA, Cardiff University's institutional repository:https://orca.cardiff.ac.uk/id/eprint/118218/

This is the author's version of a work that was submitted to / accepted for publication.

Citation for final published version:

Yahui, Zhang, Yuyin, Li and Kennedy, David 2019. An uncertain computational model for random vibration analysis of subsea pipelines subjected to spatially varying ground motions. Engineering Structures 183 , pp. 550-561. 10.1016/j.engstruct.2019.01.031

Publishers page: http://dx.doi.org/10.1016/j.engstruct.2019.01.031

Please note:
Changes made as a result of publishing processes such as copy-editing, formatting and page numbers may not be reflected in this version. For the definitive version of this publication, please refer to the published source. You are advised to consult the publisher's version if you wish to cite this paper.

This version is being made available in accordance with publisher policies. See http://orca.cf.ac.uk/policies.html for usage policies. Copyright and moral rights for publications made available in ORCA are retained by the copyright holders.

An Uncertain Computational Model for Random Vibration Analysis of Subsea Pipelines Subjected to Spatially Varying Ground Motions

Yahui Zhang[a*], Yuyin Li[a], David Kennedy[b]

[a] *State Key Laboratory of Structural Analysis for Industrial Equipment, Department of Engineering Mechanics, International Center for Computational Mechanics, Dalian University of Technology, Dalian 116023, PR China;*

[b] *School of Engineering, Cardiff University, Cardiff CF24 3AA, Wales, UK*

Corresponding author:

Dr. Y. H. Zhang

State Key Laboratory of Structural Analysis for Industrial Equipment, Department of Engineering Mechanics, Dalian University of Technology, Dalian 116023, PR China

Email: zhangyh@dlut.edu.cn

Tel: +86 411 84706337

Fax: +86 411 84708393

Abstract

Based on a nonparametric modelling approach, this paper presents a random vibration analysis of a subsea pipeline subjected to spatially varying ground motions. The earthquake-induced ground motions are modelled as nonstationary random processes and their spatial variations are considered. The modelling uncertainties of the subsea pipeline are taken into account using a random matrix theory, while the unilateral contact relationship between the pipeline and seabed is also considered. Thus, an uncertain computational model for the subsea pipeline subjected to a random earthquake is established, and the corresponding solutions are calculated using Monte Carlo simulation (MCS). In order to highlight the contribution of the unilateral contact effect to random responses of pipelines, comparative studies are performed between the unilateral and permanent contact models. In numerical examples, the possible convergence problems in the present computational model are firstly studied to determine the optimal numbers of reduced modes and MCS samples. Then influences of the randomness in the earthquake and modelling uncertainties in the pipeline are investigated qualitatively through three representative cases. The different propagations of randomness and modelling uncertainties in the unilateral and permanent models are also examined and discussed. It is concluded that the randomness of the earthquake and modelling uncertainties of the pipeline have significant influences on the statistical characteristics of earthquake responses of the pipeline.

Keywords: modelling uncertainty; random earthquake; subsea pipeline; spatially varying ground motions; unilateral contact

1 Introduction

The subsea pipeline is an important part of offshore oil and gas exploitation systems. When a pipeline is broken, the ocean environment might be polluted and underwater repair is very difficult and costly. Earthquakes are typical environmental excitations during the service life of the pipeline. As an occasional random excitation, an earthquake poses a tremendous threat to the safety of the pipeline, and hence the dynamic problem of the pipeline under an earthquake has received great attention. Due to the high cost and technical difficulties of experiments, the earthquake analysis and design of the pipeline are mainly based on numerical simulations. Thus, establishing an accurate numerical computational model is of great significance to the earthquake analysis of the pipeline. On the other hand, there are inevitably randomness and uncertainties in this computational model on account of the natural random factors and lack of relevant data. This paper discusses how to introduce randomness and uncertainties into the computational model and how they influence the system response.

For reasons of manufacturing errors and corrosion, some physical and geometric parameters of the pipeline, such as Young's modulus, mass density, wall thickness etc., may be uncertain. These parameters can be considered as random variables and their uncertainties are usually characterized by probability distribution functions. Spatial

correlations of these parameters can be further considered by using the random field theory. Uncertainties introduced by random variables or fields are called data uncertainties and this quantification approach is usually termed the parametric uncertainty approach. This approach has been successfully applied to model uncertainties in many different static and dynamic structural analyses [1-5]. Meanwhile, there is another kind of uncertainty, known as modelling uncertainty, in the dynamic analysis of the pipeline. The modelling uncertainty stems primarily from two sources. The first source is the simplifying assumptions invoked when developing a mathematical model. For instance, when dealing with a beam structure, the use of beam theory instead of three dimensional elasticity theory introduces a reduced admissible displacement field. The second source is the unquantified errors associated with the modelling of structural joints or connections. For example, the pipeline consists of many welding points and bolted connections, whose properties are always uncertain and depend on many parameters. Since the modelling uncertainty contains too many uncertain parameters, some of which cannot even be identified, it is difficult to quantify it by the parametric uncertainty approach.

To deal with the modelling uncertainty, a nonparametric approach based on random matrix theory was developed by Soize [6]. In the framework of the nonparametric approach, the generalized mass, damping and stiffness matrices of the reduced matrix model are replaced by corresponding random matrices. Then the probability distribution functions of these random matrices are constructed using Jaynes' entropy with the

constraints defined by some available information. For random matrix models of the system, it is not necessary to identify which system parameters are uncertain or their detailed distribution information, while the global dispersion level of each random matrix can be controlled by a unique positive parameter called the dispersion parameter. Hence, this approach is very suitable for dealing with the modelling uncertainty introduced by the unavoidable approximation and simplification of unknown and imprecise expression of a complex structure in establishing a mathematical equation from a physical structure. The main theoretical concepts and derivation procedures of the nonparametric approach are presented in [6, 7]. This approach is also validated by several experiments, such as a model consisting of two rectangular plates connected together with a complex joint [8, 9], a cantilever plate with randomly attached spring-mass oscillators [10], post-buckling of a thin cylindrical shell submitted to a static shear load [11], and so on. To date, this approach has been applied to various industrial problems, for example the random vibration and reliability analysis of complex aerospace engineering systems [12, 13], the dynamic behaviour prediction of an uncertain Jeffcott rotor with disc offset [14], the vibration analysis of a drill-string with bit-rock interaction [15], and so on. To the authors' knowledge, the literature contains many studies on the data uncertainty but far fewer on the modelling uncertainty, and so the focus of this paper is on modelling uncertainty in the dynamic analysis of subsea pipelines.

The data and modelling uncertainties mentioned above come from the structure itself.

Nevertheless, ground motions caused by the earthquake are also uncertain due to the natural randomness of soil and the complex propagation mechanism of earthquake waves. Uncertainties of the earthquake are usually characterized by random processes [16]. Meanwhile, spatial variations can be found in earthquake waves propagating along long-span structures, such as subsea pipelines, which result in differences in the amplitude and phase of ground motions at the supports of the structures. This phenomenon is known as spatially varying ground motions [17]. Such spatial variations have been considered in earthquake analysis of many long-span structures, such as a multi-supported suspension bridge [18], supporting towers of overhead electricity transmission systems [19], dam-reservoir-foundation systems [20], etc., and their influences on the random earthquake responses of long-span structures are recognized to be significant.

In the dynamic analysis of subsea pipelines, one key point is how to consider the relationship between pipelines and the seabed as exactly as possible. For reasons of high costs and construction difficulties, subsea pipelines always rest freely on the seabed, rather than being buried or anchored. In the literature on the dynamic analysis of unburied pipelines, pipelines are usually modelled as beams permanently contacted with elastic foundations [21-25]. However, in reality unburied pipelines are constrained unilaterally by the seabed, which means that the reaction of the seabed can only be compressive and not tensile. Hence, during the vibration of pipelines, particularly when the deformation takes place predominantly in the vertical plane, a separation of pipelines and the seabed

will occur. Clearly, the elastic foundation beam model will overestimate the constraint between pipelines and the seabed. To overcome this drawback of the elastic foundation beam model, a unilateral contact model is used in this paper to simulate the relationship between subsea pipelines and the seabed. Note that the unilateral contact model will inevitably introduce nonlinearity into the random analysis, and hence Monte Carlo simulation (MCS) seems to be the best and only method to obtain random responses of pipelines. Fortunately, the implementation of the nonparametric approach mentioned above is based on MCS, and so the contact nonlinearity does not incur any additional computational requirements.

This paper studies the random vibration of subsea pipelines subjected to spatially varying ground motions, considering the randomness of the earthquake and the modelling uncertainties of the pipeline. The paper is organized as follows. Section 2 gives the mathematical formulation of a subsea pipeline under an earthquake, and then presents the finite element model and the corresponding reduced computational model. In section 3, quantification approaches and simulation strategies for modelling uncertainties of the pipeline are given. Section 4 presents some numerical examples. Convergence analyses are firstly performed with respect to the dimension of the reduced models and the number of MCS samples. Then propagations of randomness and modelling uncertainties in the present computational model are investigated qualitatively through three representative cases. Finally, concluding remarks are made in section 5.

2 Deterministic modelling of the subsea pipeline subjected to ground motions

2.1 Governing equations of the pipeline

Fig. 1 shows a typical subsea pipeline subjected to an earthquake. The dashed part represents the initial profile of the subsea pipeline and seabed before the earthquake, while the solid part represents the deformed profile during the earthquake.

The subsea pipeline is simplified as a Timoshenko beam, and hydrodynamic forces caused by the internal oil and the surrounding sea water are considered. According to the fluid-conveying beam theory [26] and Morison's equation for slender cylindrical structures [27], governing equations of the subsea pipeline in the vertical plane can be written as

$$
\begin{gathered}
(\rho I + \rho_{\mathrm{oil}} I_{\mathrm{oil}}) \frac{\partial^2 \theta}{\partial t^2} - EI \frac{\partial^2 \theta}{\partial x^2} - \kappa GA \left(\frac{\partial w}{\partial x} - \theta \right) = 0 \\
\left(m_{\mathrm{pipe}} + m_{\mathrm{oil}} + m_{\mathrm{water}} \right) \frac{\partial^2 w}{\partial t^2} + \left(m_{\mathrm{oil}} v_{\mathrm{oil}}^2 + N_0 - \kappa GA \right) \frac{\partial^2 w}{\partial x^2} \\
+ 2 m_{\mathrm{oil}} v_{\mathrm{oil}} \frac{\partial^2 w}{\partial x \partial t} + \kappa GA \frac{\partial \theta}{\partial x} = -f_{\mathrm{seabed}}
\end{gathered}
\tag{1}
$$

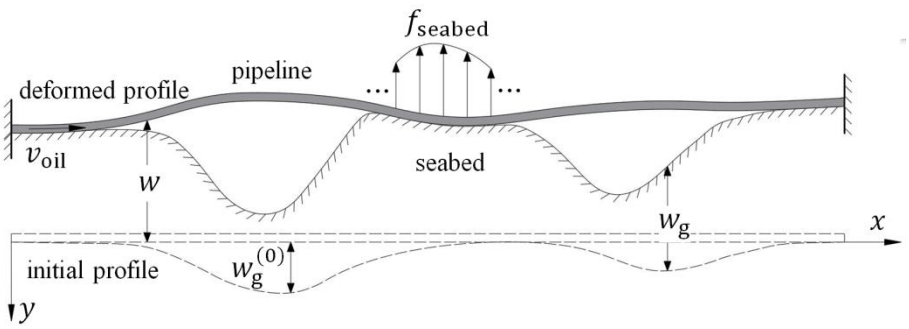

Fig. 1 Schematic of subsea pipeline and seabed

where x and t are respectively the position and time; θ and w are respectively the cross-section rotation and vertical displacement of the pipeline; ρI and $\rho_{\mathrm{oil}} I_{\mathrm{oil}}$ are respectively the moments of inertia of the pipeline and oil; EI and κGA are respectively the flexural and effective shear rigidity of the pipeline; m_{pipe}, m_{oil} and m_{water} are the masses of the pipeline, oil and additional water per unit length; v_{oil} is the flow velocity of the oil which is assumed to be a constant; N_0 is the axial compression; f_{seabed} is the reaction force per unit length of the seabed.

Ignoring the friction of the seabed and considering unilateral contact of the seabed and pipeline, the reaction force of the seabed f_{seabed} can be expressed as

$$f_{\mathrm{seabed}} = \begin{cases} 0 & \xi > 0 \\ \eta k_{\mathrm{seabed}} & \xi = 0 \end{cases} \tag{2}$$

where k_{seabed} is the stiffness of the seabed, and

$$\xi = \eta + w_{\mathrm{g}}^{(0)} + w_{\mathrm{g}} - w \tag{3}$$

is the relative displacement between the pipeline and seabed, $w_{\mathrm{g}}^{(0)}$ is the initial seabed profile, η is the compressional deformation of the seabed and w_{g} is the motion of the seabed.

2.2 Discretization by finite elements

Due to the contact nonlinearity, it is very difficult to obtain an analytical solution of Eq. (1). Hence, a numerical solution using the finite element method seems to be the only

choice. Timoshenko beam elements with two nodes are used to discretize the pipeline. Since effects of the oil conveyed through the pipeline and the surrounding seawater are considered, the beam element used in this paper is different from the conventional one. Therefore, a brief derivation of the finite element formulation is given here.

The displacement field within a beam element can be interpolated as [28]

$$w = \boldsymbol{N}\boldsymbol{q}_{\mathrm{e}}, \qquad \theta = \bar{\boldsymbol{N}}\boldsymbol{q}_{\mathrm{e}} \tag{4}$$

in which $\boldsymbol{q}_{\mathrm{e}}$ is the 4×1 node displacement vector, $\boldsymbol{N}$ and $\bar{\boldsymbol{N}}$ denote 1×4 shape function vectors, which can be written as

$$\begin{aligned} \boldsymbol{N} &= [N_1 \quad N_2 \quad N_3 \quad N_4] \\ \bar{\boldsymbol{N}} &= [\bar{N}_1 \quad \bar{N}_2 \quad \bar{N}_3 \quad \bar{N}_4] \end{aligned} \tag{5}$$

where

$$\begin{aligned} N_1 &= 1 - \frac{1}{l(l^2+12g)}(12g\chi + 3l\chi^2 - 2\chi^3) \\ N_2 &= \frac{1}{l(l^2+12g)}[(l^2+6g)l\chi - (2l^2+6g)\chi^2 + l\chi^3] \\ N_3 &= \frac{1}{l(l^2+12g)}(12g\chi + 3l\chi^2 - 2\chi^3) \\ N_4 &= \frac{1}{l(l^2+12g)}[-6gl\chi + (6g - l^2)\chi^2 + l\chi^3] \\ \bar{N}_1 &= \frac{1}{l(l^2+12g)}(6\chi^2 - 6l\chi) \\ \bar{N}_2 &= \frac{1}{l(l^2+12g)}[l^3 + 12gl - (4l^2+12g)\chi + 3l\chi^2] \\ \bar{N}_3 &= \frac{1}{l(l^2+12g)}(6l\chi - 6\chi^2) \end{aligned} \tag{6}$$

$$\bar{N}_4 = \frac{1}{l(l^2+12g)}[3l\chi^2 - (2l^2 - 12g)\chi]$$

where l is the element length, χ is the local coordinate and $g = EI/(\kappa GA)$.

The shear strain of the beam cross section can be written as

$$\gamma = \frac{\partial w}{\partial x} - \theta \tag{7}$$

Hence the strain energy and kinetic energy of a beam element can be expressed as

$$V_{\mathrm{e}} = \frac{1}{2}\int_0^a \left[EI\left(\frac{\partial\theta}{\partial x}\right)^2 + \kappa GA\gamma^2 + N_0\left(\frac{\partial w}{\partial x}\right)^2\right]\mathrm{d}\,\chi$$

$$T_{\mathrm{e}} = \frac{1}{2}\int_0^a \left[(\rho I + \rho_{\mathrm{oil}} I_{\mathrm{oil}})\left(\frac{\partial\theta}{\partial t}\right)^2 + (m_{\mathrm{pipe}} + m_{\mathrm{water}})\left(\frac{\partial w}{\partial t}\right)^2 + m_{\mathrm{oil}} v_{\mathrm{oil}}^2 + m_{\mathrm{oil}}\left(\frac{\partial w}{\partial t} + v_{\mathrm{oil}}\frac{\partial w}{\partial x}\right)^2\right]\mathrm{d}\,\chi \tag{8}$$

According to the variational principle, the element matrices can be obtained directly by substituting Eq. (4) into Eq. (8),

$$\begin{aligned}
\boldsymbol{K}_{\mathrm{e}} &= \int_0^a \left[EI\bar{\boldsymbol{N}}_\chi^{\mathrm{T}}\bar{\boldsymbol{N}}_\chi + \kappa GA(\bar{\boldsymbol{N}}_\chi^{\mathrm{T}} - \bar{\boldsymbol{N}})(\boldsymbol{N}_\chi - \bar{\boldsymbol{N}}) - m_{\mathrm{oil}} v_{\mathrm{oil}}^2 \boldsymbol{N}_\chi^{\mathrm{T}}\boldsymbol{N}_\chi\right]\mathrm{d}\,\chi \\
\boldsymbol{M}_{\mathrm{e}} &= \int_0^a \left[(m_{\mathrm{pipe}} + m_{\mathrm{oil}} + m_{\mathrm{water}})\boldsymbol{N}^{\mathrm{T}}\boldsymbol{N} + (\rho I + \rho_{\mathrm{oil}} I_{\mathrm{oil}})\bar{\boldsymbol{N}}^{\mathrm{T}}\bar{\boldsymbol{N}}\right]\mathrm{d}\,\chi \\
\boldsymbol{C}_{\mathrm{e1}} &= \int_0^a (\boldsymbol{N}^{\mathrm{T}}\boldsymbol{N}_\chi - \boldsymbol{N}_\chi^{\mathrm{T}}\boldsymbol{N})\mathrm{d}\,\chi
\end{aligned} \tag{9}$$

in which $\boldsymbol{N}_\chi = \partial\boldsymbol{N}/\partial\chi$ and $\bar{\boldsymbol{N}}_\chi = \partial\bar{\boldsymbol{N}}/\partial\chi$, superscript "T" denotes transposition, $\boldsymbol{K}_{\mathrm{e}}$ and $\boldsymbol{M}_{\mathrm{e}}$ are element stiffness and mass matrices, respectively. $\boldsymbol{C}_{\mathrm{e1}}$ is the gyroscopic

damping matrix due to the conveyed oil. Rayleigh damping is also considered here, and hence the element damping matrix can be expressed as

$$\boldsymbol{C}_{\mathrm{e}} = \boldsymbol{C}_{\mathrm{e1}} + d_1\boldsymbol{M}_{\mathrm{e}} + d_2\boldsymbol{K}_{\mathrm{e}} \tag{10}$$

where d_1 and d_2 are Rayleigh damping factors corresponding to the mass and stiffness, respectively.

The subsea pipeline is discretized into N Timoshenko beam elements, while the seabed is discretized into $N-2$ spring elements, as shown in Fig. 2. The discrete governing equation of the subsea pipeline can be written as

$$\boldsymbol{M}\ddot{\boldsymbol{X}} + \boldsymbol{C}\dot{\boldsymbol{X}} + \boldsymbol{K}\boldsymbol{X} = \boldsymbol{F}_{\mathrm{seabed}} \tag{11}$$

in which $\boldsymbol{M}$, $\boldsymbol{C}$ and $\boldsymbol{K}$ are structural mass, damping and stiffness matrices, respectively; $\boldsymbol{X}$ is the nodal displacement vector, $\boldsymbol{F}_{\mathrm{seabed}}$ is the reaction force vector of the seabed; and $\dot{}$ denotes differentiation with respect to time t.

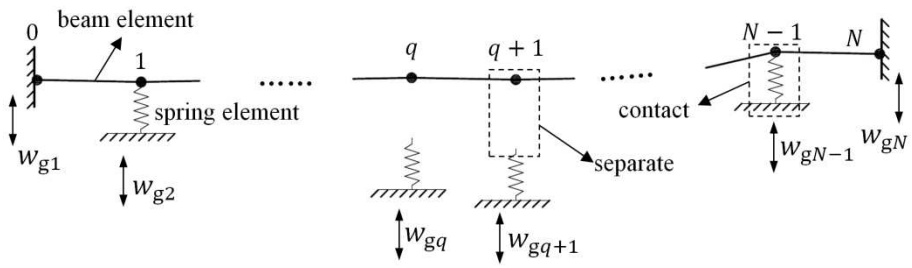

Fig. 2 Finite element model of subsea pipeline and seabed

Since the variation of earthquakes is considered, motions of different points at seabed will have differences in phases, amplitudes, or both. This means that the analysis of the subsea pipeline subjected to earthquake is a multi-support excitation problem. To solve this problem, Eq. (11) is rearranged as

$$\begin{bmatrix} \boldsymbol{M}_{\mathrm{s}} & \boldsymbol{M}_{\mathrm{sb}} \\ \boldsymbol{M}_{\mathrm{sb}}^{\mathrm{T}} & \boldsymbol{M}_{\mathrm{b}} \end{bmatrix} \begin{Bmatrix} \ddot{\boldsymbol{X}}_{\mathrm{s}} \\ \ddot{\boldsymbol{X}}_{\mathrm{b}} \end{Bmatrix} + \begin{bmatrix} \boldsymbol{C}_{\mathrm{s}} & \boldsymbol{C}_{\mathrm{sb}} \\ \boldsymbol{C}_{\mathrm{sb}}^{\mathrm{T}} & \boldsymbol{C}_{\mathrm{b}} \end{bmatrix} \begin{Bmatrix} \dot{\boldsymbol{X}}_{\mathrm{s}} \\ \dot{\boldsymbol{X}}_{\mathrm{b}} \end{Bmatrix} + \begin{bmatrix} \boldsymbol{K}_{\mathrm{s}} & \boldsymbol{K}_{\mathrm{sb}} \\ \boldsymbol{K}_{\mathrm{sb}}^{\mathrm{T}} & \boldsymbol{K}_{\mathrm{b}} \end{bmatrix} \begin{Bmatrix} \boldsymbol{X}_{\mathrm{s}} \\ \boldsymbol{X}_{\mathrm{b}} \end{Bmatrix} = \begin{Bmatrix} \boldsymbol{R}_{\mathrm{s}} \\ \boldsymbol{R}_{\mathrm{b}} \end{Bmatrix} \tag{12}$$

in which the subscripts “b” and “s” indicate the support and non-support degrees of freedom (DOF), respectively, so that $\boldsymbol{X}_{\mathrm{b}}$ are the enforced displacements of the supports on both sides, $\boldsymbol{X}_{\mathrm{s}}$ are all nodal displacements except those at the supports, $\boldsymbol{R}_{\mathrm{b}}$ are the enforced forces at the supports and $\boldsymbol{R}_{\mathrm{s}}$ are the reaction forces of the seabed. Expanding the first row of Eq. (12) gives

$$\boldsymbol{M}_{\mathrm{s}}\ddot{\boldsymbol{X}}_{\mathrm{s}} + \boldsymbol{C}_{\mathrm{s}}\dot{\boldsymbol{X}}_{\mathrm{s}} + \boldsymbol{K}_{\mathrm{s}}\boldsymbol{X}_{\mathrm{s}} = \boldsymbol{R}_{\mathrm{s}} + \boldsymbol{P} \tag{13}$$

in which $\boldsymbol{P} = -\boldsymbol{M}_{\mathrm{sb}}\ddot{\boldsymbol{X}}_{\mathrm{b}} - \boldsymbol{C}_{\mathrm{sb}}\dot{\boldsymbol{X}}_{\mathrm{b}} - \boldsymbol{K}_{\mathrm{sb}}\boldsymbol{X}_{\mathrm{b}}$ is the effective earthquake force acting on the non-support DOF.

Each node of the beam element used in this paper has two DOF, namely translation and rotation in the vertical plane. However, the reaction force of the seabed is assumed to act only on the translation DOF and not the rotation DOF of the pipeline during the contact. Combining Eqs. (2) and (3), the reaction force $\boldsymbol{R}_{\mathrm{s}}$ can be expressed as

$$
\begin{aligned}
&\boldsymbol{R}_{\mathrm{s}} = \mathbb{D}\boldsymbol{R} \\
&\boldsymbol{R}_q = \begin{cases} 0 & \boldsymbol{\xi}_q > 0 \\ -K_{\mathrm{seabed}}\boldsymbol{\eta}_q & \boldsymbol{\xi}_q = 0 \end{cases} \\
&\boldsymbol{\xi}_q = \boldsymbol{w}_q - \boldsymbol{\eta}_q - \boldsymbol{w}_{\mathrm{g}q}^{(0)} - \boldsymbol{w}_{\mathrm{g}q} \\
&q = 1,2,\cdots,N-1
\end{aligned} \tag{14}
$$

where $\boldsymbol{R}$ is the N_{ns}-dimensional reaction force vector and N_{ns} is the number of non-support nodes, $\mathbb{D}$ is the translation DOF indicator matrix with "0" and "1" elements, $\boldsymbol{\xi}$ is the relative displacement vector between the pipeline and seabed model, $\boldsymbol{w}$ is the translation vector of the pipeline, K_{seabed} is the stiffness of the seabed spring, $\boldsymbol{\eta}$ is the compressional deformation vector of the seabed, $\boldsymbol{w}_{\mathrm{g}}^{(0)}$ and $\boldsymbol{w}_{\mathrm{g}}$ are respectively the profile vector and displacement vector of the seabed.

2.3 Reduced computational model

Due to the contact nonlinearity, many iterations must be performed during the solution of Eq. (13). Meanwhile, the finite element model may have a large dimension and the dynamical analysis will be time consuming. In order to reduce the computational cost, one can project the nonlinear equations onto a relative lower dimensional subspace spanned by a set of specific basis functions and then the dimension of equations can be reduced [29]. In this paper, the basis used for reduction is the natural modes of the pipeline (without the seabed). The natural modes are obtained from the following generalized eigenvalue problem

$$
\boldsymbol{K}_{\mathrm{s}}\boldsymbol{\Phi}_p = \omega_p^2\boldsymbol{M}_s\boldsymbol{\Phi}_p, \qquad p = 1,2,\cdots N_{\mathrm{mode}} \tag{15}
$$

in which ω_p and $\boldsymbol{\Phi}_p$ are the p-th natural frequency and mode of the system, respectively, N_{mode} is the dimension of $\boldsymbol{K}_{\mathrm{s}}$ and $\boldsymbol{M}_{\mathrm{s}}$. Thus, the reduced problem can be expressed as

$$\boldsymbol{X}_{\mathrm{s}} = \boldsymbol{\Phi}\boldsymbol{q} \tag{16a}$$

$$\boldsymbol{M}_{\mathrm{r}}\ddot{\boldsymbol{q}} + \boldsymbol{C}_{\mathrm{r}}\dot{\boldsymbol{q}} + \boldsymbol{K}_{\mathrm{r}}\boldsymbol{q} = \boldsymbol{r} + \boldsymbol{p} \tag{16b}$$

where

$$\begin{aligned} &\boldsymbol{\Phi} = [\boldsymbol{\Phi}_1 \quad \boldsymbol{\Phi}_2 \quad \cdots \quad \boldsymbol{\Phi}_n](n < N_{\mathrm{mode}}) \\ &\boldsymbol{M}_{\mathrm{r}} = \boldsymbol{\Phi}^{\mathrm{T}}\boldsymbol{M}_{\mathrm{s}}\boldsymbol{\Phi}, \qquad \boldsymbol{C}_{\mathrm{r}} = \boldsymbol{\Phi}^{\mathrm{T}}\boldsymbol{C}_{\mathrm{s}}\boldsymbol{\Phi}, \qquad \boldsymbol{K}_{\mathrm{r}} = \boldsymbol{\Phi}^{\mathrm{T}}\boldsymbol{K}_{\mathrm{s}}\boldsymbol{\Phi} \\ &\boldsymbol{r} = \boldsymbol{\Phi}^{\mathrm{T}}\boldsymbol{R}_{\mathrm{s}}, \qquad \boldsymbol{p} = \boldsymbol{\Phi}^{\mathrm{T}}\boldsymbol{P} \end{aligned} \tag{17}$$

It is noted that Eq. (16b) cannot be decoupled into a set of single DOF systems for two reasons. Firstly, $\boldsymbol{C}_{\mathrm{s}}$ contains the component of gyroscopic damping, which cannot be diagonalized by the natural modes. Secondly, $\boldsymbol{R}_{\mathrm{s}}$ is not known a priori and depends on the current state of the pipeline and seabed due to the contact nonlinearity. This is different from the linear case or the case without internal oil.

3 Uncertain modelling of the earthquake and the pipeline

Two different kinds of uncertainties are considered in the present computational model. The first one is randomness of the earthquake and is modelled as a random process. The other one is modelling uncertainties of the pipeline, for which the random matrix theory is applied to model them.

3.1 Random earthquake with spatial variation

Assuming that the acceleration of the ground motion during the earthquake is a nonstationary random process, it can be expressed as

$$\ddot{w}_{\mathrm{g}} = g(t)\ddot{d}(t) \tag{18}$$

in which $\ddot{d}(t)$ is a stationary and homogeneous Gaussian random process with zero mean value and its auto power spectral density (PSD) is $S_0(\omega)$, ω is the circular frequency, $g(t)$ is a slowly varying deterministic envelope function. Then the cross-PSD of the acceleration at two arbitrary points can be expressed as

$$S\ (\Delta x, \omega) = \gamma(\Delta x, \omega) S_0(\omega) \tag{19}$$

where $\Delta x = |x_i - x_j|$ is the distance between the two points x_i and x_j on the ground, and $\gamma(\Delta x, \omega)$ is the coherency function which represents the spatial variation of earthquakes.

Considering n separate points on the ground, the auto-PSD matrix of the ground acceleration at these points has the form

$$\mathbf{S}(\omega) = \begin{bmatrix} \gamma_{11}(\omega) & \gamma_{12}(\omega) & \cdots & \gamma_{1n}(\omega) \\ \gamma_{21}(\omega) & \gamma_{22}(\omega) & \cdots & \gamma_{2n}(\omega) \\ \vdots & \vdots & \ddots & \vdots \\ \gamma_{n1}(\omega) & \gamma_{nn}(\omega) & \cdots & \gamma_{nn}(\omega) \end{bmatrix} S_0(\omega) \tag{20}$$

where $\gamma_{ij}(\omega)(i, j = 1,2, \cdots n)$ is the coherency function of x_i and x_j. By using

Cholesky decomposition, $\mathbf{S}(\omega)$ can be represented as the product of a lower triangular matrix $\mathbf{H}(\omega)$ and its Hermitian transpose, i.e.

$$\mathbf{S}(\omega) = \mathbf{H}(\omega)\mathbf{H}^{\mathrm{H}}(\omega) \tag{21}$$

The stationary time history sample of the acceleration at point x_i is obtained in the following terms as a summation of cosine functions with random phase angles [30]

$$\ddot{d}_i(t) = 2\sum_{l=1}^{i}\sum_{m=1}^{N_{\mathrm{freq}}} |H_{il}(\omega_m)|\sqrt{\Delta\omega}\cos(\omega_m t - \theta_{il}(\omega_m) + \Phi_{lm}) \tag{22}$$

where $H_{il}(\omega_m)$ is the element on the i-th row and l-th column of matrix $\mathbf{H}(\omega_m)$, $\Delta\omega = \omega_{\mathrm{cut}}/N$ is the frequency step, ω_{cut} is the cut off frequency, N is the number of frequency steps, N_{freq} is the number of frequencies, $\omega_m = m\Delta\omega$ is the m-th frequency, $\theta_{il}(\omega_m)$ is the phase of $H_{il}(\omega_m)$, and Φ_{lm} is the random phase angle distributed uniformly between 0 and 2π. The corresponding nonstationary time history sample can then be obtained according to Eq. (18). The reader is referred to [31] for a more detailed illustration of the simulation procedure of random earthquakes with spatial variations.

3.2 Nonparametric modelling for uncertainties of the pipeline

As mentioned in the introduction, the nonparametric approach developed by Soize [6] is able to take into account modelling uncertainties in the computational model. This subsection will show the main theories and derivations of the nonparametric approach

and more details can be found in [6, 7].

The uncertainties of mass, damping and stiffness matrices are considered and these matrices are replaced by the corresponding random matrices. Thus the governing equations shown in Eq. (16b) can be rewritten as

$$\boldsymbol{M}_{\mathrm{r}}^{\mathrm{npar}}\ddot{\boldsymbol{q}} + \boldsymbol{C}_{\mathrm{r}}^{\mathrm{npar}}\dot{\boldsymbol{q}} + \boldsymbol{K}_{\mathrm{r}}^{\mathrm{npar}}\boldsymbol{q} = \boldsymbol{r} + \boldsymbol{p} \tag{23}$$

where $\boldsymbol{M}_{\mathrm{r}}^{\mathrm{npar}}$, $\boldsymbol{C}_{\mathrm{r}}^{\mathrm{npar}}$, $\boldsymbol{K}_{\mathrm{r}}^{\mathrm{npar}}$ are $n \times n$ symmetric positive-definite random matrices corresponding to the mass, damping and stiffness, respectively.

According to the random matrix theory [6], $p_{\boldsymbol{A}}$, the probability density function of the random matrix $\boldsymbol{A}\left(\boldsymbol{A} \in \boldsymbol{M}_{\mathrm{r}}^{\mathrm{npar}}, \boldsymbol{C}_{\mathrm{r}}^{\mathrm{npar}}, \boldsymbol{K}_{\mathrm{r}}^{\mathrm{npar}}\right)$, yields the following constraint conditions

$$\begin{cases} \displaystyle\int_{\mathbb{M}_n^+(\mathbb{R})} p_{\boldsymbol{A}}(\boldsymbol{A})\tilde{\mathrm{d}}\boldsymbol{A} = 1 \\ \displaystyle\int_{\mathbb{M}_n^+(\mathbb{R})} \boldsymbol{A} p_{\boldsymbol{A}}(\boldsymbol{A})\tilde{\mathrm{d}}\boldsymbol{A} = \underline{\boldsymbol{A}} \in \mathbb{M}_n^+(\mathbb{R}) \\ \displaystyle\int_{\mathbb{M}_n^+(\mathbb{R})} \ln\left(\det(\boldsymbol{A})\right) p_{\boldsymbol{A}}(\boldsymbol{A})\tilde{\mathrm{d}}\boldsymbol{A} = v \quad \text{with } |v| < +\infty \end{cases} \tag{24}$$

where $\mathbb{M}_n^+(\mathbb{R})$ indicates the subspace constituted of all the positive-definite symmetric real matrices with $n \times n$ dimensions, $\tilde{\mathrm{d}}\boldsymbol{A} = 2^{n(n-1)/4}\prod_{1\le i\le j\le n}\mathrm{d}\boldsymbol{A}_{ij}$ and $\underline{\boldsymbol{A}}$ is the mean value of the random matrix $\boldsymbol{A}$. Taking into account the constraint conditions in Eq. (24) and using the Maximum Entropy Principle, the probability density function of $\boldsymbol{A}$ can be deduced as

$$p_{\boldsymbol{A}}(\boldsymbol{A}) = \mathbb{I}_{\mathbb{M}_n^+(\mathbb{R})}(\boldsymbol{A}) \times c_{\boldsymbol{A}} \times \left(\det(\boldsymbol{A})\right)^{\lambda-1} \times \exp\left(-\frac{(n-1+2\lambda)}{2}\mathrm{tr}\{\underline{\boldsymbol{A}}^{-1}\boldsymbol{A}^{\mathrm{T}}\}\right) \tag{25}$$

where $\mathbb{I}_{\mathbb{M}_n^+(\mathbb{R})}(\boldsymbol{A})$ is the indicator function, which is equal to 1 when $\boldsymbol{A} \in \mathbb{M}_n^+(\mathbb{R})$ and 0 otherwise, $c_{\boldsymbol{A}}$ is a positive constant which can be expressed as

$$c_{\boldsymbol{A}} = \frac{(2\pi)^{-n(n-1)/4}\left(\frac{n-1+2\lambda}{2}\right)^{n(n-1+2\lambda)/2}}{\left\{\prod_{l=1}^{n}\Gamma\left(\frac{n-l+2\lambda}{2}\right)\right\}\left(\det(\underline{\boldsymbol{A}})\right)^{(n-1+2\lambda)/2}} \tag{26}$$

where $\Gamma(x) = \int_0^{+\infty} t^{x-1}\mathrm{e}^{-t}\,\mathrm{d}t (x > 0)$ is the gamma function.

The variance of the component $\boldsymbol{A}_{jk}$ which is at the j-th row and k-th column of matrix $\boldsymbol{A}$ can be calculated from

$$\sigma_{jk} = \frac{1}{n-1+2\lambda}\left(\underline{\boldsymbol{A}}_{jk}^2 + \underline{\boldsymbol{A}}_{jj}\underline{\boldsymbol{A}}_{kk}\right), \qquad 0 < j \le k \le n \tag{27}$$

Note that $\mathrm{E}\left\{\left\|\boldsymbol{A} - \underline{\boldsymbol{A}}\right\|_{\mathrm{F}}^2\right\} = \sum_j \sum_k \sigma_{jk}^2$, in which $\|\boldsymbol{A}\|_{\mathrm{F}}^2 = \left(\mathrm{tr}(\boldsymbol{A}\boldsymbol{A}^*)\right)^{1/2}$ is the Frobenius norm of the matrix $\boldsymbol{A}$, $\boldsymbol{A}^*$ is the conjugate of the matrix $\boldsymbol{A}$ and $\mathrm{tr}(\quad)$ denotes the trace. Thus the dispersion parameter of the matrix $\boldsymbol{A}$ can be defined as

$$\delta_{\boldsymbol{A}} = \left\{\frac{\mathrm{E}\left\{\left\|\boldsymbol{A} - \underline{\boldsymbol{A}}\right\|_{\mathrm{F}}^2\right\}}{\left\|\underline{\boldsymbol{A}}\right\|_{\mathrm{F}}^2}\right\}^{\frac{1}{2}} = \left\{\frac{1}{n-1+2\lambda}\left(1 + \frac{\left(\mathrm{tr}(\underline{\boldsymbol{A}})\right)^2}{\left(\mathrm{tr}(\underline{\boldsymbol{A}}^2)\right)}\right)\right\}^{\frac{1}{2}} \tag{28}$$

Then the parameter λ in Eqs. (25) to (28) can be calculated by

$$\lambda = \frac{1}{2\delta_A^2}\left(1 - \delta_A^2(n-1) + \frac{\left(\mathrm{tr}(\underline{\boldsymbol{A}})\right)^2}{\left(\mathrm{tr}(\underline{\boldsymbol{A}}^2)\right)}\right) \tag{29}$$

From the above derivation, it can be seen that once the dimension n has been determined, $\delta_{\boldsymbol{A}}$ controls the dispersion level of the random matrix $\boldsymbol{A}$ and hence is called the "dispersion parameter". It is proved that $\delta_{\boldsymbol{A}}$ should satisfy the following constraint

$$0 < \delta_{\boldsymbol{A}} < \sqrt{\frac{n+1}{n+5}} \tag{30}$$

Given a dispersion parameter $\delta_{\boldsymbol{A}}$ and mean value matrix $\underline{\boldsymbol{A}}$, samples of the random matrix $\boldsymbol{A}$ can then be generated. Since $\boldsymbol{A}$ is a positive-definite symmetric matrix, it can be written as

$$\boldsymbol{A} = \underline{\boldsymbol{L}}_{\boldsymbol{A}}^{\mathrm{T}}\boldsymbol{G}\underline{\boldsymbol{L}}_{\boldsymbol{A}} \tag{31}$$

in which, $\underline{\boldsymbol{L}}_{\boldsymbol{A}}$ is an upper triangular matrix obtained by applying the Cholesky factorization to $\underline{\boldsymbol{A}}$, i.e., $\underline{\boldsymbol{A}} = \underline{\boldsymbol{L}}_{\boldsymbol{A}}^{\mathrm{T}}\underline{\boldsymbol{L}}_{\boldsymbol{A}}$, $\boldsymbol{G}$ is a random matrix and whose mean value is a n-dimensional identity matrix. The random matrix $\boldsymbol{G}$ is further written as

$$\boldsymbol{G} = \boldsymbol{L}_{\boldsymbol{G}}^{\mathrm{T}}\boldsymbol{L}_{\boldsymbol{G}} \tag{32}$$

where $\boldsymbol{L}_{\boldsymbol{G}}$ is an upper triangular random matrix resulting from the Cholesky factorization and its samples can be generated by the following steps [12]:

(1) random variables $\boldsymbol{L}_{jk}(j \le k)$ are assumed to be independent;

(2) for a non-diagonal element, i.e. $j < k$, the real-valued random variable $\boldsymbol{L}_{\boldsymbol{G}jk}$ can be rewritten as $\boldsymbol{L}_{\boldsymbol{G}jk} = \sigma_n \left| U_{jk} \right|$, in which $\sigma_n = \delta_{\boldsymbol{A}}(n+1)^{-1/2}$ and U_{jk} is a Gaussian random variable with zero mean and variance of 1;

(3) for a diagonal element, i.e. $j = k$, the positive-valued random variable $\boldsymbol{L}_{\boldsymbol{G}jk}$ can be rewritten as $\boldsymbol{L}_{\boldsymbol{G}jj} = \sigma_n \sqrt{2V_j}$ in which σ_n is defined in step (2) and V_j is a gamma random variable with the following probability density function

$$p_{V_j}(v) = \mathbb{I}_{\mathbb{M}_n^+(\mathbb{R})}(v) \frac{1}{\Gamma(\alpha_{n,j})} v^{\alpha_{n,j}-1} \mathrm{e}^{-v}, \qquad \alpha_{n,j} = \frac{n+1}{2\delta_{\boldsymbol{A}}^2} + \frac{1-j}{2} \tag{33}$$

4 Numerical examples

The physical and geometric parameters of the subsea pipeline are taken as follows: Young's modulus $E = 207 \times 10^9 \mathrm{Pa}$, mass density $\rho = 7850\,\mathrm{kg/m^3}$, Poisson's ratio $\nu = 0.3$, Rayleigh damping factors corresponding to the stiffness $d_1 = 0.05$ and the mass $d_2 = 0.01$, total length of pipeline $L_0 = 100\mathrm{m}$, shear correction factor $\kappa = 2(1+\nu)/(4+3\nu)$, outer radius $R_{\mathrm{out}} = 0.6\mathrm{m}$, wall thickness $h = 0.017\mathrm{m}$. The mass densities of the oil in the pipeline and surrounding water are $\rho_{\mathrm{oil}} = 800\,\mathrm{kg/m^3}$ and $\rho_{\mathrm{water}} = 1025\,\mathrm{kg/m}$, respectively, and the velocity of the oil is $v_{\mathrm{oil}} = 3\,\mathrm{m/s}$.

According to the design standard [32], the effective axial compression N_0 should not exceed $0.5N_{\mathrm{cr}}$, where N_{cr} is the critical buckling load, and hence $N_0 = 0.3N_{\mathrm{cr}}$ is used in this paper. The pipeline is discretized into 100 elements and both ends are simply supported.

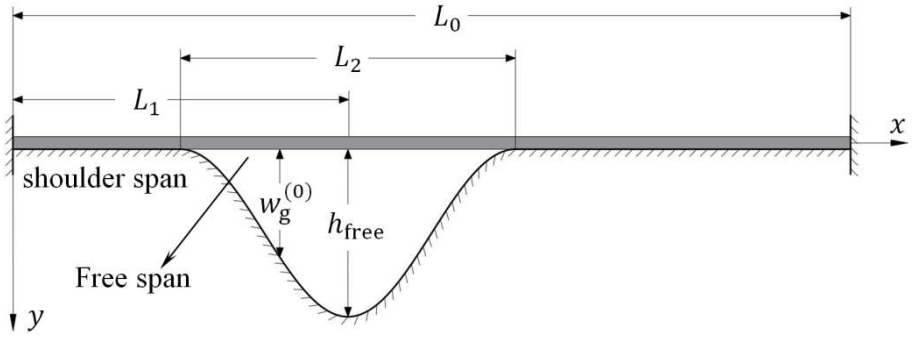

Fig. 3 Schematic of seabed profile

A seabed profile shown in Fig. 3 is considered. The middle point of the free span is $L_1 = 50\text{m}$, the length is $L_2 = 50\text{m}$, the maximum depth is $h_{\text{free}} = 0.3\text{m}$. The depth distribution of the free span is represented approximately by a cosine function, hence the seabed profile can be expressed as

$$w_g^{(0)} = \begin{cases} 0 & 0 \le x < L_1 - L_2/2 \\ \dfrac{h_{\text{free}}}{2}\left[1 - \cos\dfrac{2\pi(x - L_1 + L_2/2)}{L_2}\right] & L_1 - L_2/2 \le x < L_1 + L_2/2 \\ 0 & L_1 + L_2/2 \le x \le L_0 \end{cases} \quad (34)$$

A ground acceleration spectrum power density function developed by Clough and Penzien [33] is used here, and the corresponding parameters are $S_g = 0.018\,\text{m}^2/\text{s}^3$, $\omega_g = 15\,\text{rad/s}$, $\omega_f = 0.1\omega_g$, $v_{\text{app}} = 1000\,\text{m/s}$, $\xi_g = \xi_f = 0.6$ [34]. The duration of the earthquake is $T = 10.92\text{s}$, and the time step for the numerical integration is $\Delta t = 0.01\text{s}$, hence the number of time steps is $N_t = 1093$. The nonstationary modulation function and spatial variation parameters of earthquake can be found in [31]. Samples of ground acceleration are generated by Eqs. (18) and (22), and then a correction scheme suggested by Berg and Housner [35] is used to eliminate the baseline offsets caused by

the accumulation of random noise in accelerations.

In this section, the optimal numbers of reduced modes and MCS samples are firstly determined through convergence analysis. Then, the propagations of randomness of the earthquake and modelling uncertainties of the seabed are investigated. Since the unilateral contact of the pipeline and seabed introduces nonlinearity into the computational model, the randomness and modelling uncertainties may have some different influences on random responses. Hence, a model of permanent contact between the pipeline and seabed is also used for a comparative study. It is noted that in the permanent contact model, the system stiffness matrix contains two components, namely, the pipeline and seabed. However, to be consistent with the unilateral contact model, only the pipeline is assumed to be uncertain while the seabed is assumed to be deterministic.

4.1 Convergence analysis

The convergence problem of the number of reduced modes is studied based on the mean model of the system, and the excitation is an arbitrary sample of the ground motions. The study uses the following convergence function

$$\mathrm{Conv}(n_b) = \int_0^T \|\boldsymbol{w}(t, n_b)\|^2 \mathrm{d}t \tag{35}$$

in which $\boldsymbol{w}(t, n_b)$ is the displacement vector of the pipeline at time t by using the first n_b natural modes as reduced modes. For the convenience of comparing the cases of unilateral and permanent contact on a same figure, results are normalized by those with

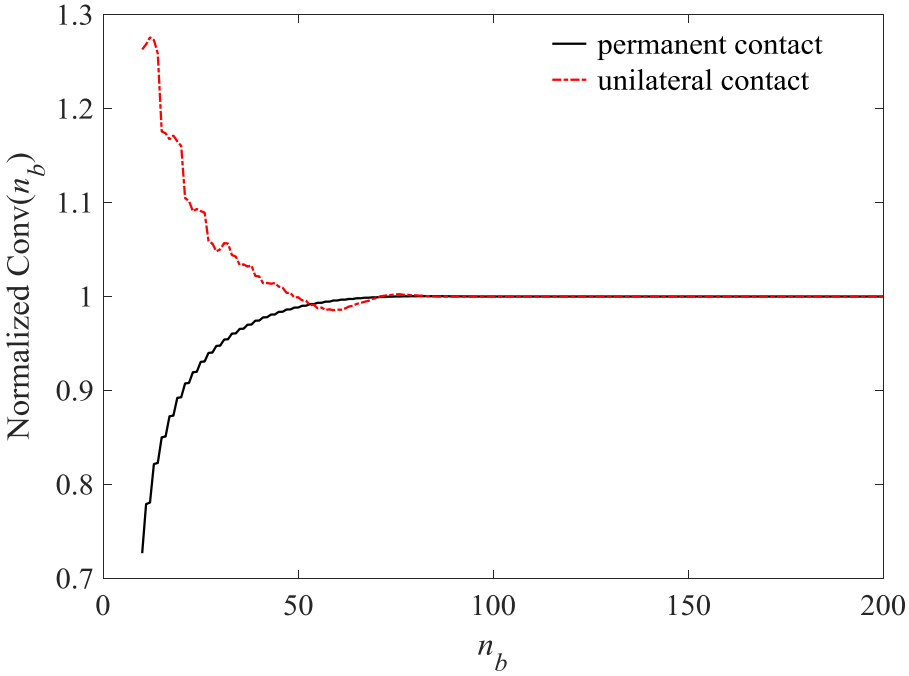

Fig. 4 Normalized convergence results for reduced modes in permanent and unilateral contact models

$n_b = 200$, which is the case without any reduction. Fig. 4 gives the convergence results, which indicate that both unilateral and permanent contact models will obtain convergent results when $n_b \geq 80$. Hence, $n_b = 80$ is used in the subsequent analysis.

On the other hand, since the random results are obtained by MCS, it is necessary to study the convergence of MCS samples. The corresponding convergence function can be defined as [36]

$$\mathrm{Conv}(n_s) = \frac{1}{n_s}\sum_{i=1}^{n_s}\int_0^T \|\boldsymbol{w}(t, s_i)\|^2 \mathrm{d}t \tag{31}$$

where $\boldsymbol{w}(t, s_i)$ indicates the displacement vector of the pipeline for the i-th sample at time t and n_s is the total number of samples. The convergence results for cases with

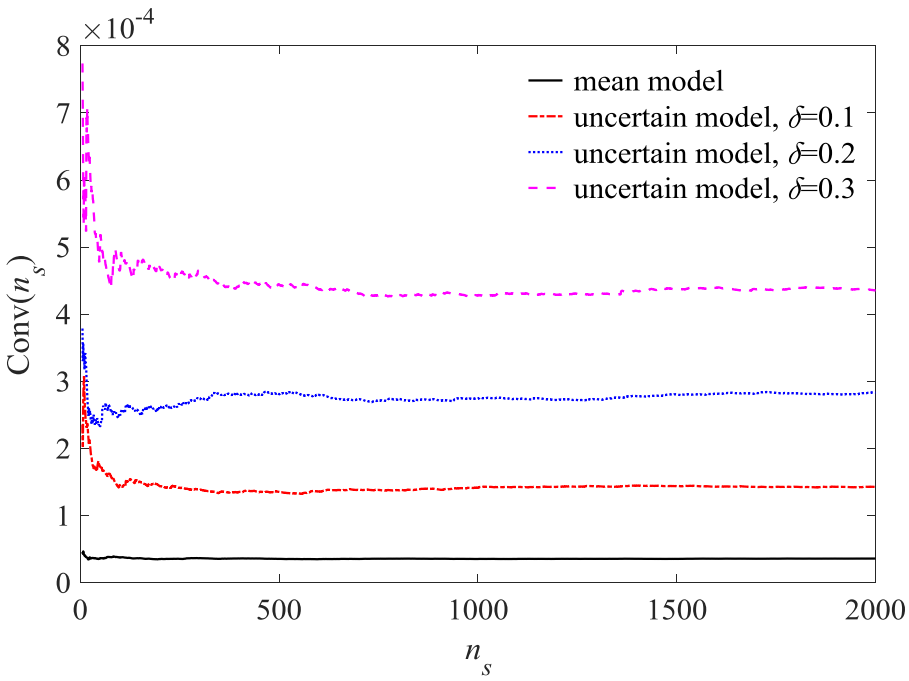

(a) Permanent contact model

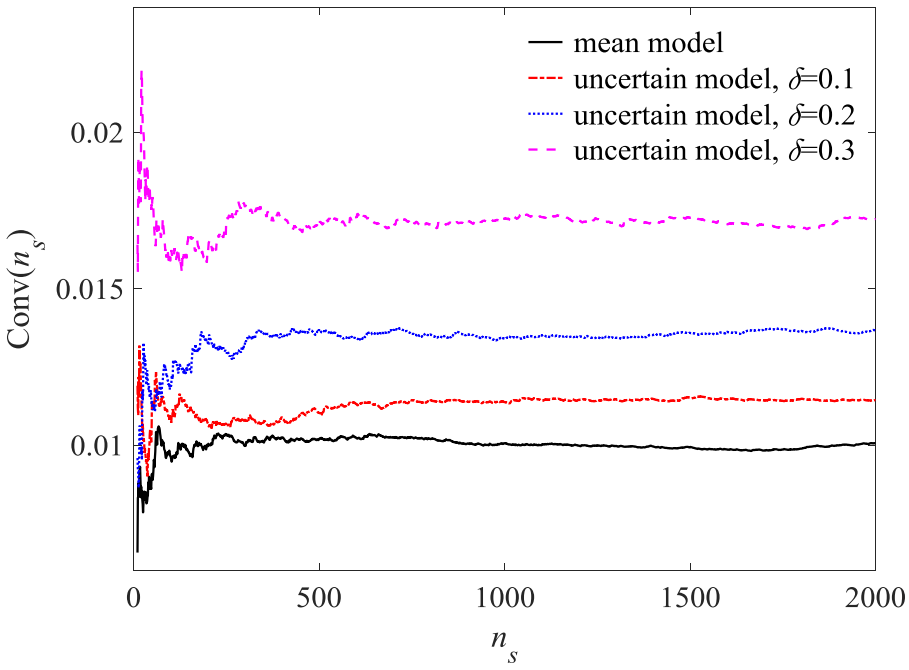

(b) Unilateral contact model

Fig. 5 Convergence results for numbers of Monte Carlo simulation in permanent and unilateral contact models

different dispersion parameters, i.e., $\delta_M = \delta_K = 0.1,\ 0.2,\ 0.3$, are calculated and shown in Fig. 5. It can be seen that the permanent contact model appears to have a faster convergence with the number of samples than the unilateral contact model. To balance the accuracy and efficiency, $n_s = 1000$ is used in following studies. It is worth noting that the number of MCS samples is always chosen to be in the range of about 200 to 1500 in the relevant literature [6-14, 36].

4.2 Propagations of randomness and modelling uncertainties

In the present computational model, two kinds of uncertainty, namely, the randomness of ground motions and modelling uncertainties of the pipeline are included. To study the propagations of these uncertainties qualitatively, three representative cases with different uncertainties are considered and their details are shown in Table 1.

Table. 1 Three representative cases with different uncertainties

	Ground motions	Pipeline
Case 1	Deterministic Arbitrary sample	Modelling uncertainties Random matrix
Case 2	Randomness Random process	Deterministic Mean model
Case 3	Randomness Random process	Modelling uncertainties Random matrix

4.2.1 Case 1: deterministic ground motions and uncertain pipeline model

To study the influences of modelling uncertainties on random responses, the case with deterministic ground motions and an uncertain pipeline model is carried out firstly. The ground motion is an arbitrary sample generated by the approach in subsection 3.1. Time histories of this sample at $x = 50\text{m}$ are given in Fig. 6.

Fig. 7 displays the time-varying mean values of displacements of the pipeline at $x = 50\text{m}$ for cases with different dispersion parameters. It is shown that the dispersion parameters of modelling uncertainties have slight influences on the mean values of responses in the permanent contact model. However these influences are very significant in the unilateral contact model, giving larger mean values as the dispersion parameters are increased. Fig. 8 gives the time-varying standard deviations of displacement responses at the same location. It can be seen that standard deviations increase with dispersion parameters in both the permanent and unilateral contact models. However, this increase is almost linear in the permanent contact model, while it is clearly nonlinear in the unilateral contact model. These results demonstrate that the modelling uncertainties of the pipeline have significantly different propagation in linear and nonlinear systems.

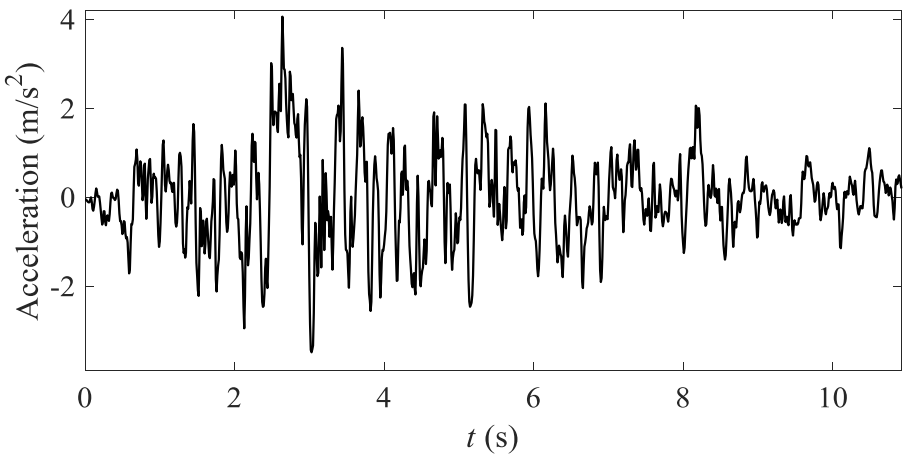

(a) Acceleration

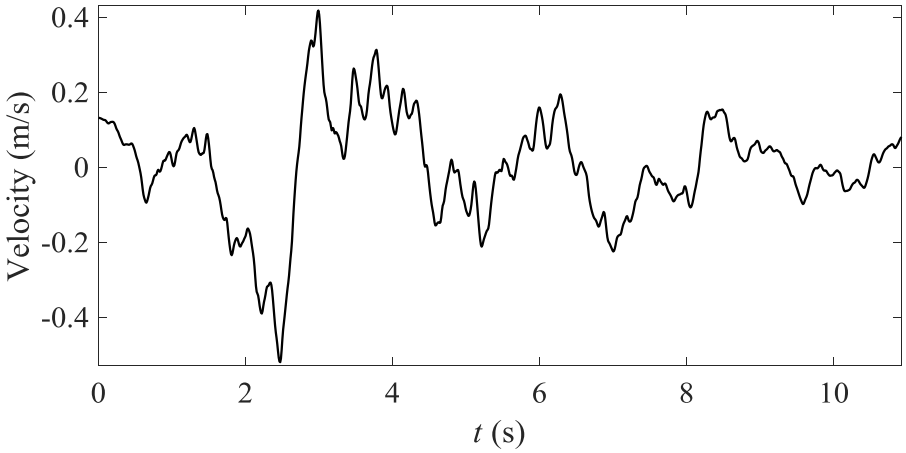

(b) Velocity

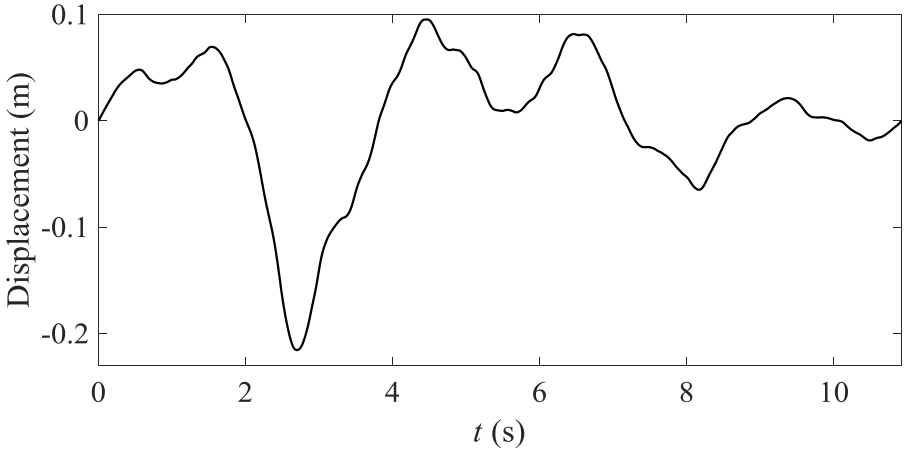

(c) Displacement

Fig. 6 Time histories of the ground motion at $x = 50$m

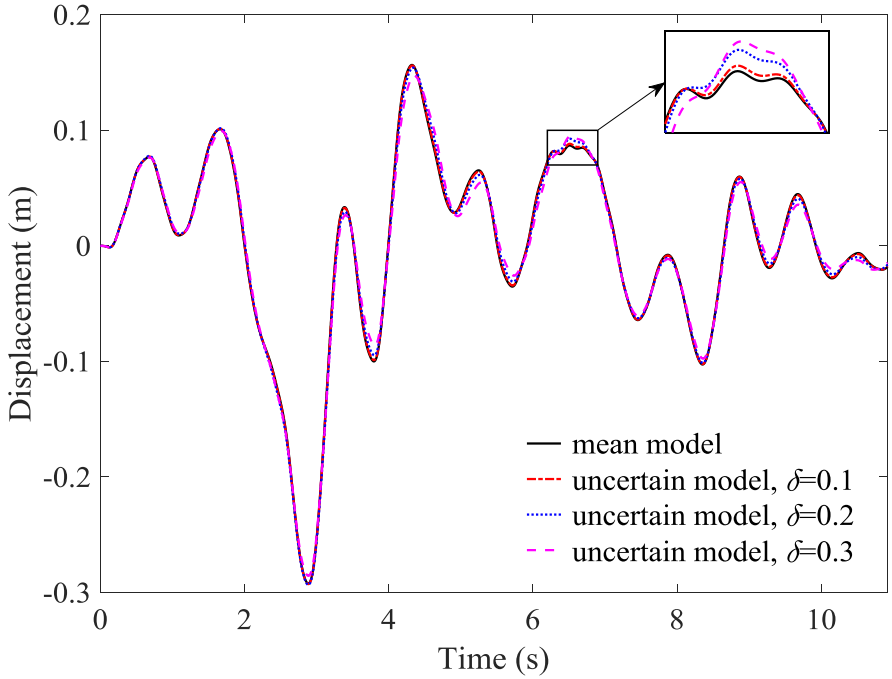

(a) Permanent contact model

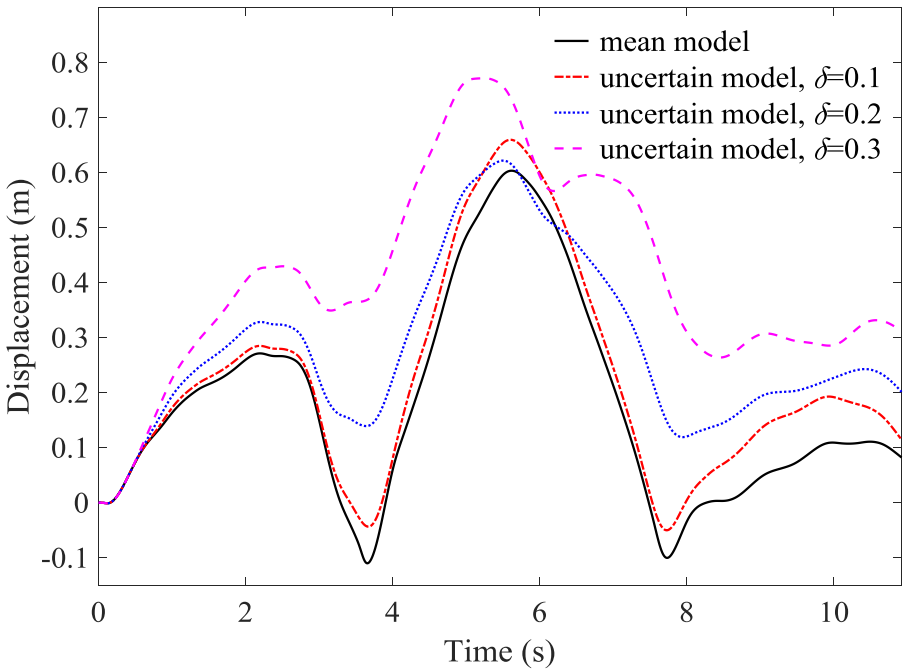

(b) Unilateral contact model

Fig. 7 Mean values of pipeline displacements for the case of deterministic ground motions and uncertain pipeline model

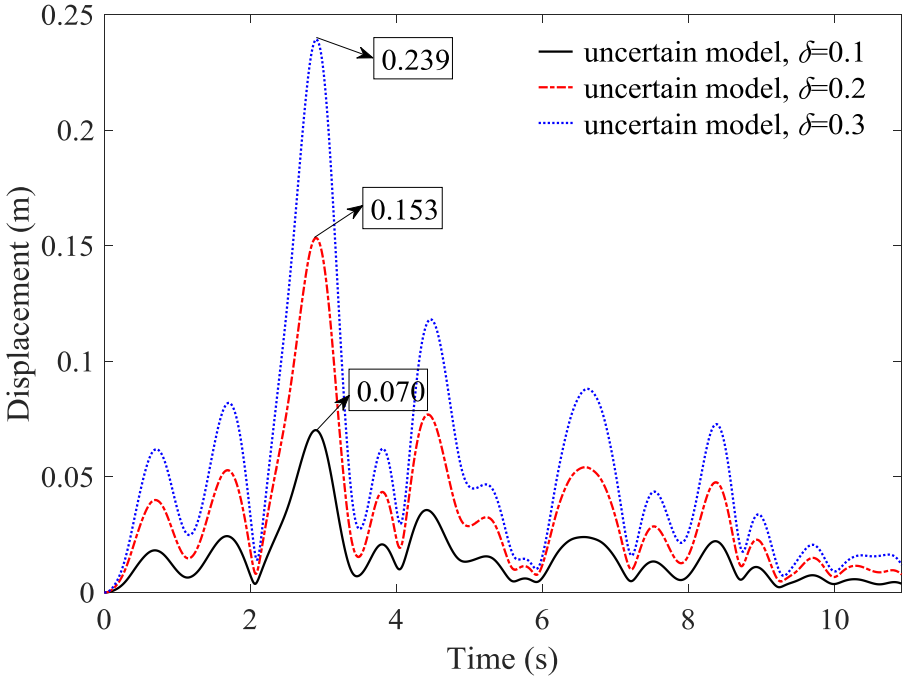

(a) Permanent contact model

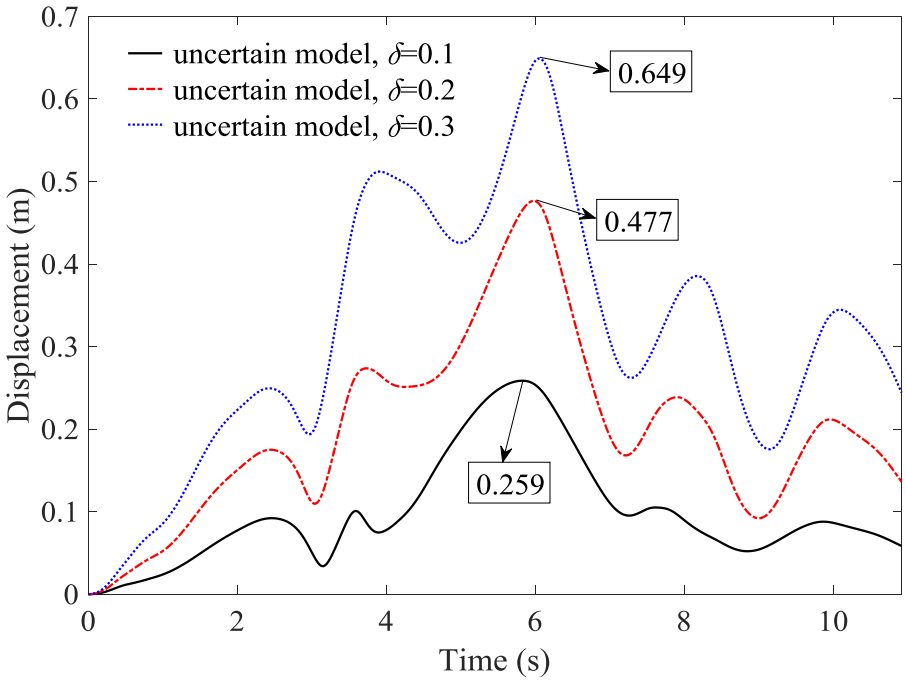

(b) Unilateral contact model

Fig. 8 Standard deviations of pipeline displacements for the case of deterministic ground motions and uncertain pipeline model

4.2.2 Case 2: random ground motions and deterministic pipeline

In this subsection, a computational model with random ground motions and deterministic pipeline model is adopted to study the propagation of randomness of the earthquake. Note that the ground motions are assumed to be Gaussian distributed with zero mean.

Fig. 9 presents the time-varying statistical moments of displacements of the pipeline at $x = 50\text{m}$ in the permanent and unilateral contact models. It can be seen from Fig. 9(a) that the responses have zero mean values in the permanent contact model while much larger mean values in the unilateral contact model. The reason is that for a linear and time-invariant system (the permanent contact model), if the input has zero mean, then the output also has zero mean. However, in the unilateral contact model which is a nonlinear

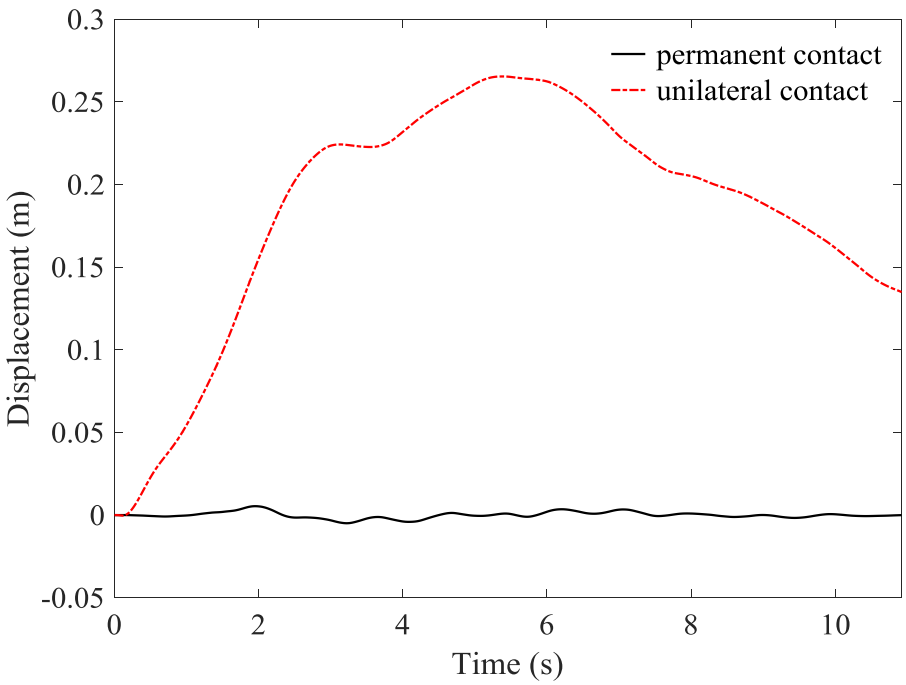

(a) Mean values

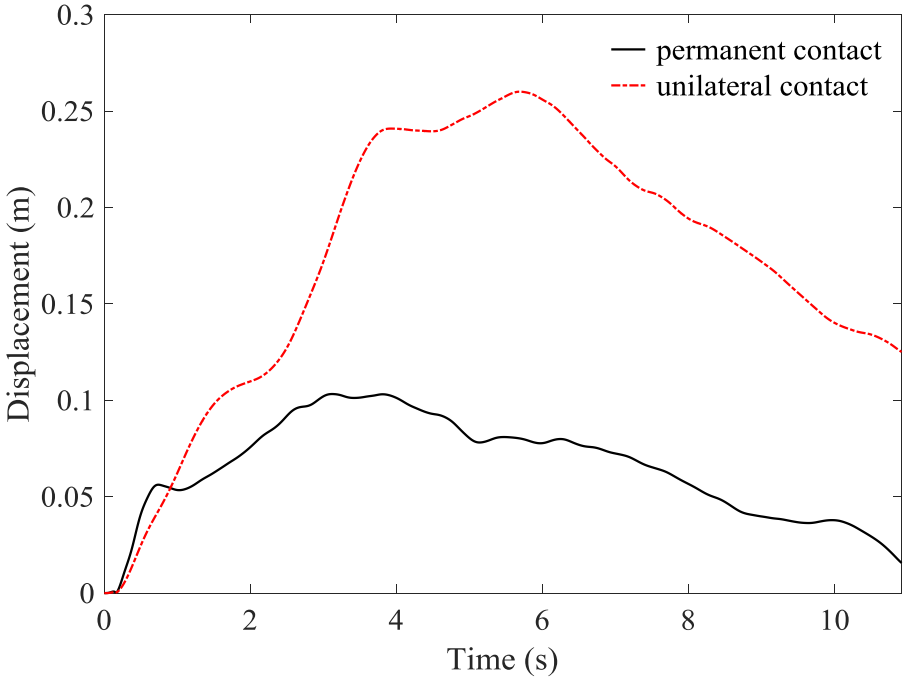

(b) Standard deviations

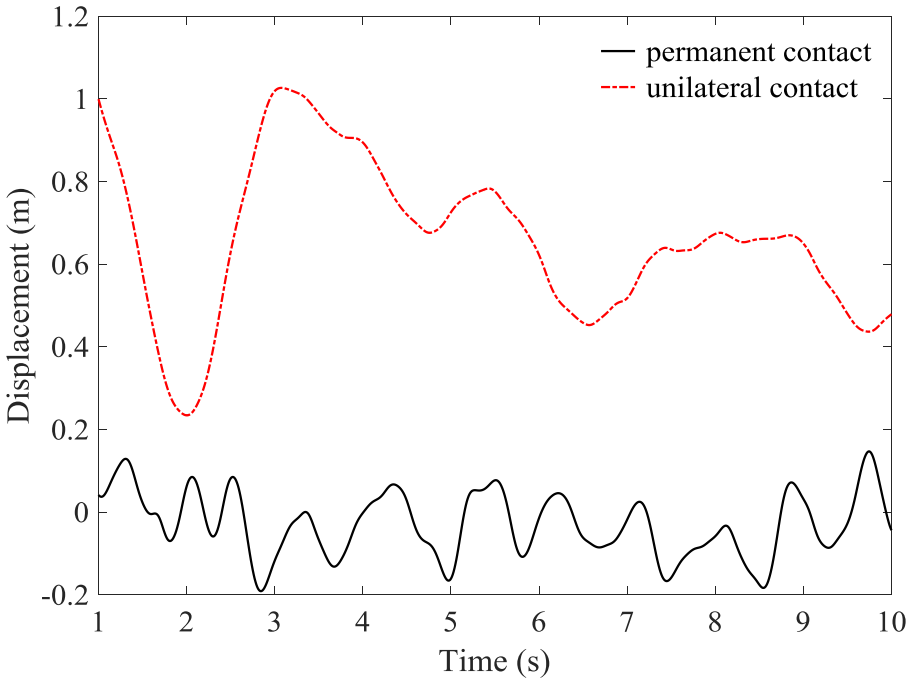

(c) Skewnesses

Fig. 9 Statistical moments of pipeline displacements for the case of random ground motions and deterministic pipeline model

system, the responses have non-zero mean values even if the excitation has zero mean values. Fig. 9(b) gives the standard deviations. It is observed that the standard deviations in the unilateral contact model are much larger than those in the permanent contact model, except for a short time at the beginning of the earthquake. The skewness, which is a measure of the asymmetry from the Gaussian distribution, is given in Fig. 9(c). It can be seen that both skewnesses fluctuate around zero, with a small amplitude in the permanent contact model but relatively large values in the unilateral contact model. This phenomenon indicates that when the ground motions are Gaussian, the responses of the permanent contact are also Gaussian while those of the unilateral contact models are not. Based on these results, it is concluded that the randomness of the ground motions propagates in different ways in the permanent and unilateral contact models.

4.2.3 Case 3: random ground motions and uncertain pipeline

Finally, a case with random ground motions and an uncertain pipeline model is carried out to study the combined influences of the randomness and modelling uncertainties on random responses. The time-varying mean values of displacements of the pipeline at $x = 50\mathrm{m}$ are shown in Fig. 10. It can be seen that for the permanent contact model, the mean values vary in a small range around zero with amplitudes of the order 10^{-3}m, which means that random responses can be regarded as being zero mean. It is also shown that the influence of the dispersion parameter on the amplitude of mean values is not obvious in the permanent contact model. However, as shown in Fig. 10(b), the dispersion

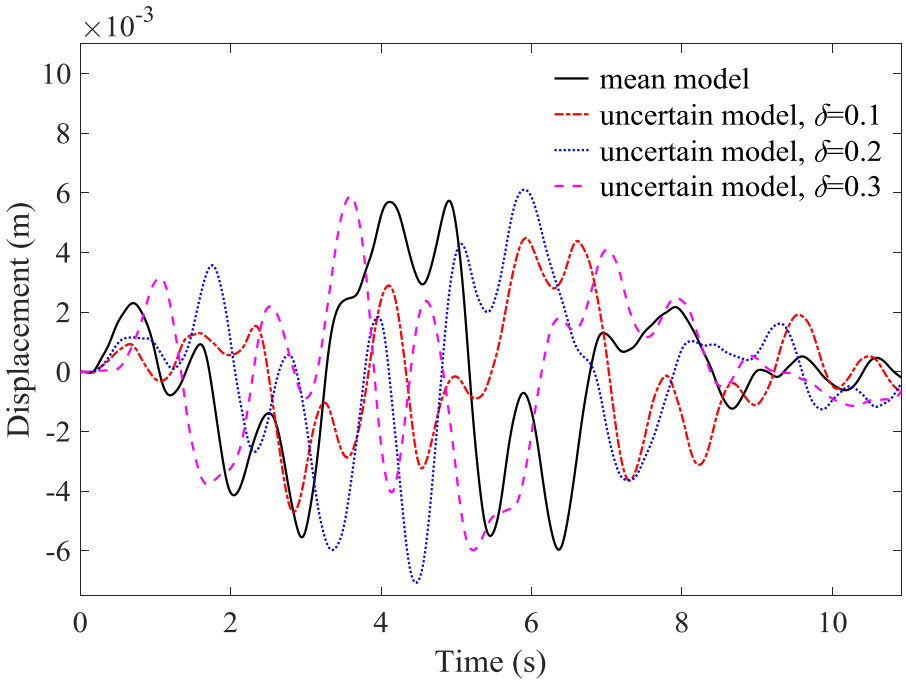

(a) Permanent contact model

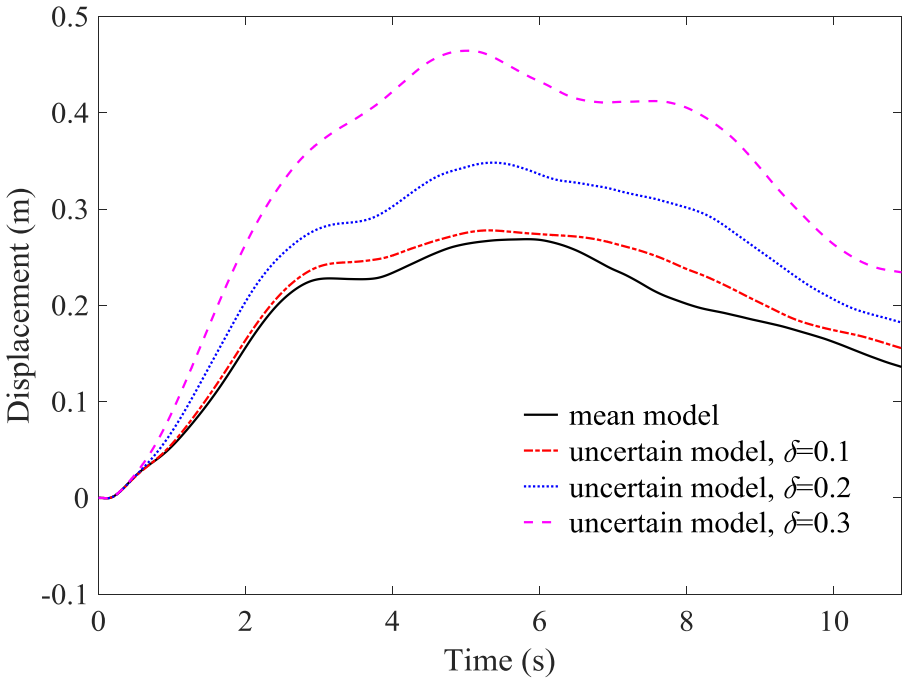

(b) Unilateral contact model

Fig. 10 Mean values of pipeline displacements for the case of random ground motions and uncertain pipeline model

parameter has a remarkable influence on the mean values for the unilateral contact model. Fig. 11 shows the time-varying standard deviations of displacement responses and the characteristics of results are quite similar to those in Fig. 8. However, the standard deviations in Fig. 11 do not increase linearly with the dispersion parameter any more for the permanent contact model, in contrast to those in Fig. 8. Compared to the results for Cases 1 and 2, it can be concluded that the consideration of both randomness and modelling uncertainty will make random responses more dispersed than the cases in which either one is not considered.

The reliability assessment of structures subjected to an earthquake is usually formulated as a first passage problem, i.e. the probability that the structural response exceeds a given threshold. Based on certain assumptions, the first passage problem is usually reduced to finding the statistical moments of the maximum response during a specified period. Figs. 12 and 13 give mean values and standard deviations of maximum displacement responses of the pipeline, respectively. It is shown that both mean values and standard deviations tend to increase with the dispersion parameter, especially those in the middle region of the pipeline. Meanwhile, it can be seen that mean values and standard deviations near the end supports, i.e., locations $x = 0$ to 20m and $x = 80$ to 100m, vary little with the increase of the dispersion parameter in the permanent contact model (Figs. 12(a) and 13(a)), but vary greatly for the unilateral contact model (Figs. 12(b) and 13(b)). There are two reasons for this phenomenon. Firstly, the end supports of the

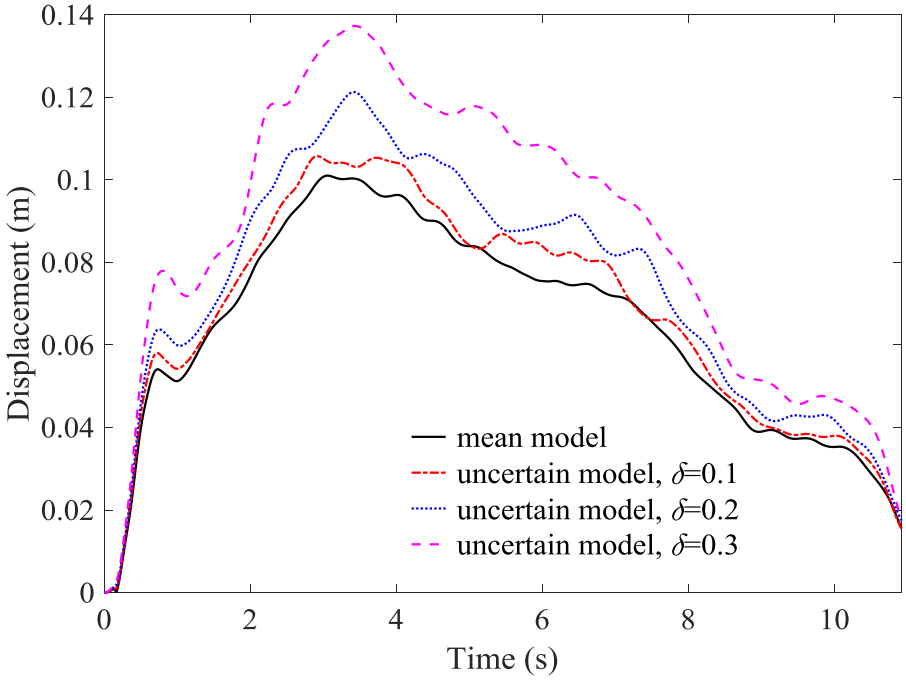

(a) Permanent contact model

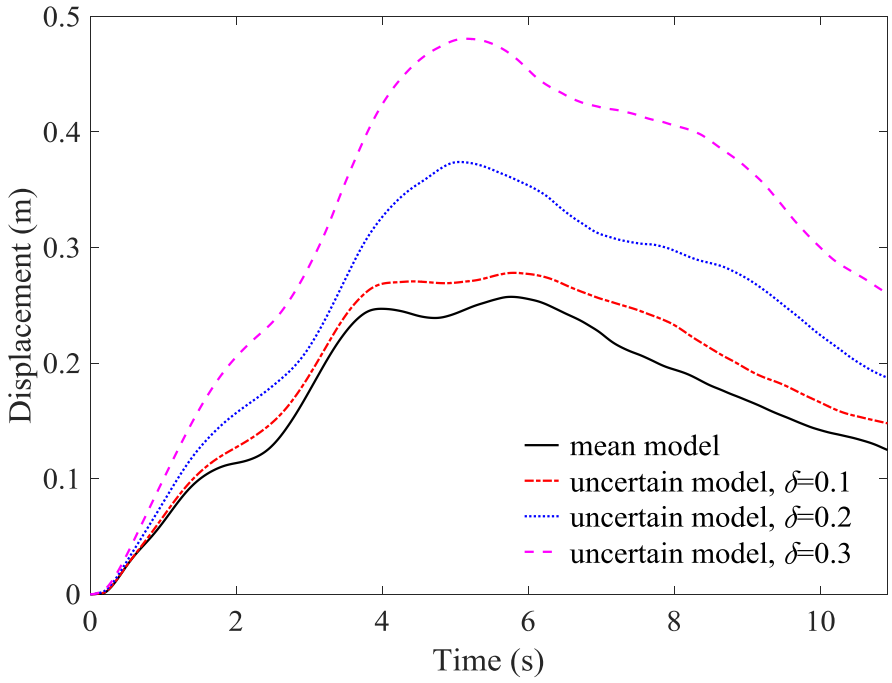

(b) Unilateral contact model

Fig. 11 Standard deviations of pipeline displacements for the case of random ground motions and uncertain pipeline model

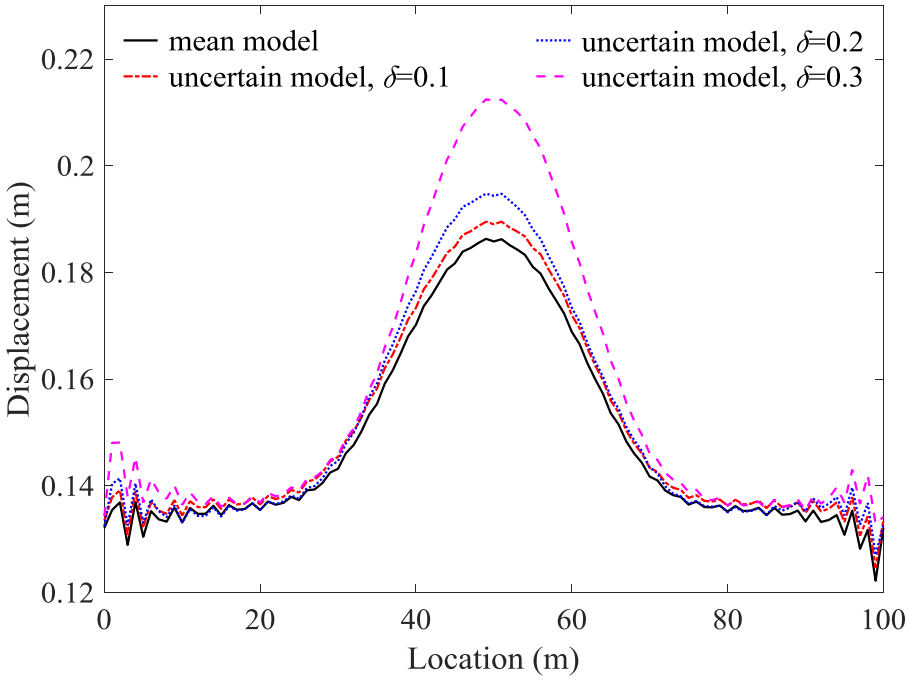

(a) Permanent contact model

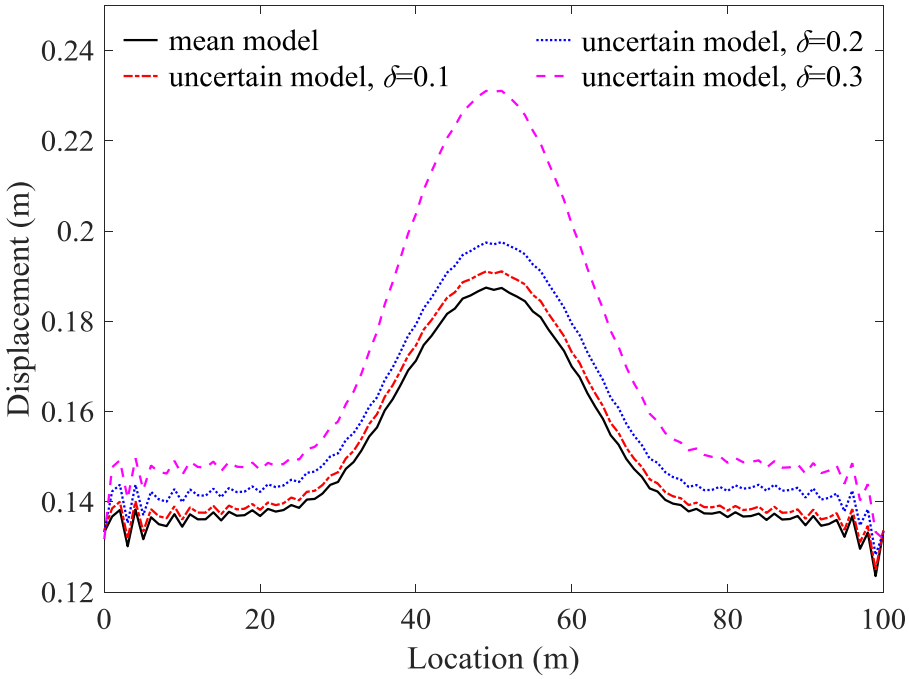

(b) Unilateral contact model

Fig. 12 Mean values of the maximum responses of the pipeline

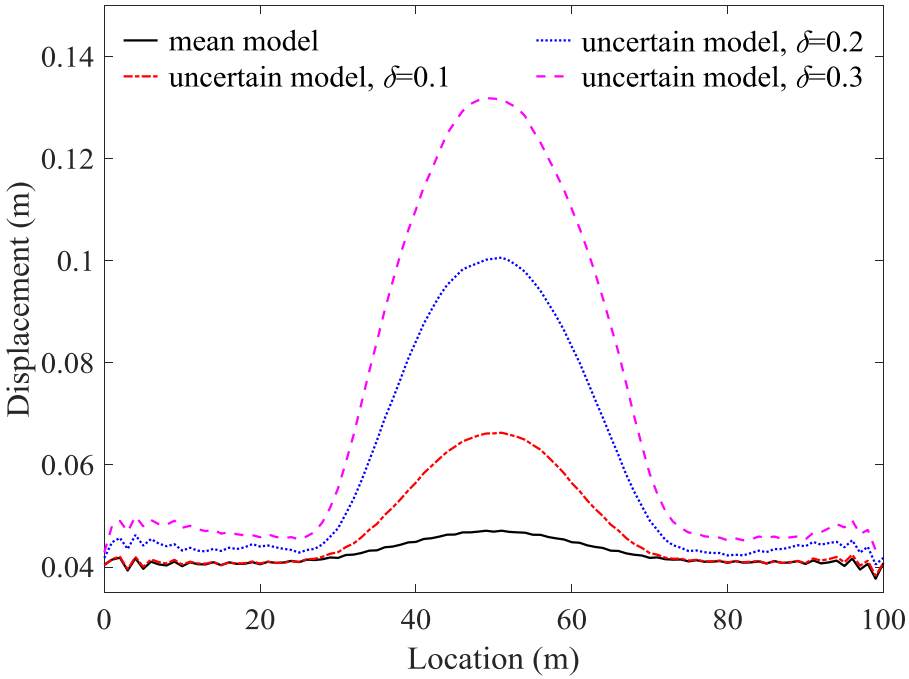

(a) Permanent contact model

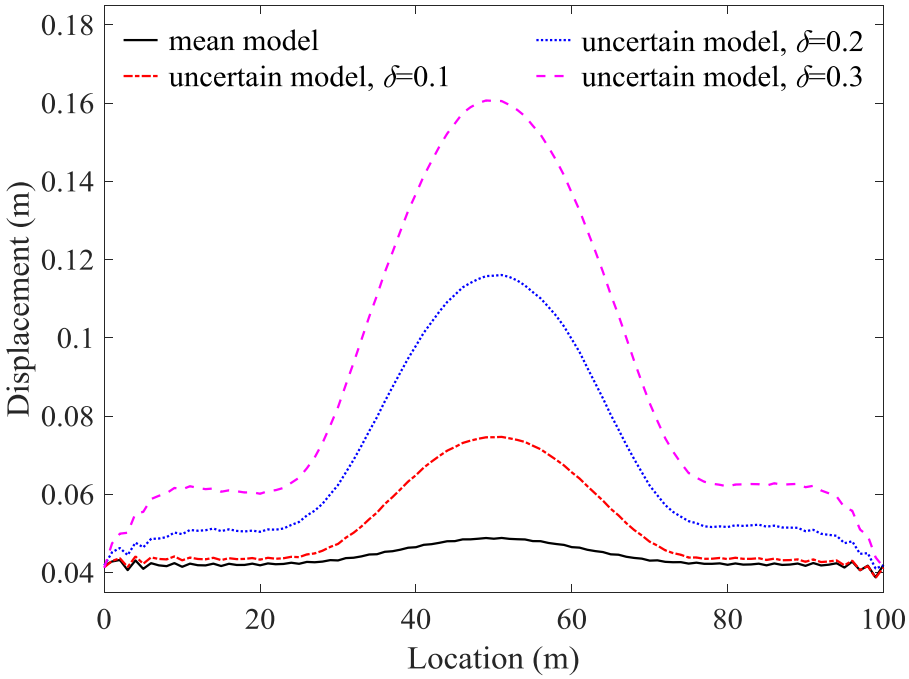

(b) Unilateral contact model

Fig. 13 Standard deviations of the maximum responses of the pipeline

pipeline are assumed to be rigid and hence their motions are equal to the ground motions, which are independent of the uncertainties of the pipeline. Secondly, the permanent contact model has a larger system stiffness than the unilateral contact model due to the total constraint of the seabed. Hence, in the permanent contact model, motions of the pipeline near the end supports are to a great extent controlled by the motions of the end supports. But in the unilateral contact model, the effect of end supports is much smaller.

5 Conclusions

This paper presents a computational model for the random vibration analysis of a subsea pipeline subjected to an earthquake. The randomness of the earthquake and modelling uncertainties of the pipeline are included in this computational model. Meanwhile, the spatial variation of the ground motions and the unilateral contact relationship between the pipeline and seabed are considered. Based on the present computational model, propagations of the randomness and modelling uncertainties are investigated through three representative cases. Results indicate that both the randomness of the earthquake and modelling uncertainties of the pipeline have significant influences on the random responses of the pipeline, and hence they should be considered in any earthquake analysis of the pipeline. Furthermore, comparative studies are performed between the permanent and unilateral contact models and remarkable differences are observed in their random responses. For the permanent contact model, random responses

of the pipeline exhibit a consistent statistical characteristic with the randomness and modelling uncertainties, whereas for the unilateral contact model random responses are more dispersed. These differences demonstrate the necessity of consideration of the unilateral contact effect in the random earthquake analysis of subsea pipelines, especially for those unburied or not anchored in deep sea regions.

Acknowledgments

This authors wish to acknowledge the financial support from the National Basic Research Program of China (2014CB046803), the National Science Foundation of China (11672060), and the Cardiff University Advanced Chinese Engineering Centre.

References

[1] Ghanem RG, Spanos PD. Stochastic Finite Element: A Spectral Approach. Springer-Verlag; 1991.

[2] Schuëller GI, Pradlwarter HJ. Uncertain linear systems in dynamics: Retrospective and recent developments by stochastic approaches. Eng Struct 2009; 31(11): 2507-2517.

[3] Stefanou G. The stochastic finite element method: past, present and future. Comput Methods Appl Mech Eng 2009; 198(9-12): 1031-1051.

[4] Singh BN, Lal A, Kumar R. Nonlinear bending response of laminated composite

plates on nonlinear elastic foundation with uncertain system properties. Eng Struct 2008; 30(4): 1101-1112.

[5] Fabro AT, Ferguson NS, Jain T, Halkyard R, Mace BR. Wave propagation in one-dimensional waveguides with slowly varying random spatially correlated variability. J Sound Vib 2015; 343(4): 20-48.

[6] Soize C. A nonparametric model of random uncertainties for reduced matrix models in structural dynamics. Probabilist Eng Mech 2000; 15(3): 277-294.

[7] Soize C. Random matrix theory and non-parametric model of random uncertainties in vibration analysis. J Sound Vib 2003; 263(4): 893-916.

[8] Chebli H, Soize C. Experimental validation of a nonparametric probabilistic model of nonhomogeneous uncertainties for dynamical systems. J Acoust Soc Am 2004; 115(2): 697-705.

[9] Duchereau J, Soize C. Transient dynamics in structures with non-homogeneous uncertainties induced by complex joints. Mech Syst Signal Process 2006; 20(4): 854-867.

[10] Adhikari S, Pastur L, Lytova A, Du Bois J. Eigenvalue density of linear stochastic dynamical systems: A random matrix approach. J Sound Vib 2012; 331(5): 1042-1058.

[11] Capiez-Lernout E, Soize C, Mignolet MP. Post-buckling nonlinear static and dynamical analyses of uncertain cylindrical shells and experimental validation.

Comput Methods Appl Mech Eng 2014; 271: 210-230.

[12] Capiez-Lernout E, Pellissetti M, Pradlwarter H, Schuëller GI, Soize C. Data and model uncertainties in complex aerospace engineering systems. J Sound Vib 2006; 295(3-5): 923-938.

[13] Pellissetti M, Capiez-Lernout E, Pradlwarter H, Soize C, Schuëller GI. Reliability analysis of a satellite structure with a parametric and a non-parametric probabilistic model. Comput Methods Appl Mech Eng 2008; 198(2): 344-357.

[14] Gan C, Wang Y, Yang S, Cao Y. Nonparametric modeling and vibration analysis of uncertain Jeffcott rotor with disc offset. Int J Mech Sci 2014; 78: 126-134.

[15] Ritto TG, Soize C, Sampaio R. Non-linear dynamics of a drill-string with uncertain model of the bit–rock interaction. Int J Nonlin Mech 2009; 44(8): 865-876.

[16] Newland DE. An Introduction to Random Vibrations, Spectral and Wavelet Analysis. Longman; 2012.

[17] Bi K, Hao H. Modelling and simulation of spatially varying earthquake ground motions at sites with varying conditions. Probabilist Eng Mech 2012; 29: 92-104.

[18] Zhang YH, Li QS, Lin JH, Williams FW. Random vibration analysis of long-span structures subjected to spatially varying ground motions. Soil Dyn Earthq Eng 2009; 29(4): 620-629.

[19] Tian L, Gai X, Qu B, Li H, Zhang P. Influence of spatial variation of ground motions on dynamic responses of supporting towers of overhead electricity transmission

systems: An experimental study. Eng Struct 2016; 128: 67-81.

[20] Bilici Y, Bayraktar A, Soyluk K, Haciefendioğlu K, Ateş Ş, Adanur S. Stochastic dynamic response of dam-reservoir-foundation systems to spatially varying earthquake ground motions. Soil Dyn Earthq Eng 2009; 29(3): 444-458.

[21] Soliman HO, Datta TK. Response of overground pipelines to random ground motion. Eng Struct 1996; 18(7): 537-545.

[22] Xu T, Lauridsen B, Bai Y. Wave-induced fatigue of multi-span pipelines. Mar Struct 1999; 12(2): 83-106.

[23] Sollund HA, Vedeld K, Fyrileiv O. Modal response of short pipeline spans on partial elastic foundations. Ocean Eng 2015; 105: 217-230.

[24] Zeinoddini M, Parke GAR, Sadrossadat SM. Free-spanning submarine pipeline response to severe ground excitations: water-pipeline interactions. J Pipeline Syst Eng Prac 2012; 3(4): 135-149.

[25] Vedeld K, Sollund H, Hellesland J. Free vibrations of free spanning offshore pipelines. Eng Struct, 2013; 56: 68-82.

[26] Païdoussis MP, Li GX. Pipes conveying fluid: a model dynamical problem. J Fluid Struct 1993; 7(2): 137-204.

[27] Morison JR, Johnson JW, Schaaf SA. The force exerted by surface waves on piles. J Petrol Technol 1950; 2(5): 149-154.

[28] Zhai H, Wu Z, Liu Y, Yue Z. Dynamic response of pipeline conveying fluid to random

excitation. Nucl Eng Des 2011; 241(8): 2744-2749.

[29] Mignolet MP, Soize C. Stochastic reduced order models for uncertain geometrically nonlinear dynamical systems. Comput Methods Appl Mech Eng 2008; 197(45-48): 3951-3963.

[30] Shinozuka M. Monte Carlo solution of structural dynamics. Comput Struct 1972; 2(5-6): 855-874.

[31] Li Y, Zhang Y, Kennedy D. Reliability analysis of subsea pipelines under spatially varying ground motions by using subset simulation. Reliab Eng Syst Saf 2018; 172: 74-83.

[32] Det Norsk Veritas. Submarine Pipeline Systems, DNV-OS-F101, 2007.

[33] Clough RW, Penzien J. Dynamics of Structures. McGraw-Hill; 1993.

[34] Dumanogluid AA, Soyluk K. A stochastic analysis of long span structures subjected to spatially varying ground motions including the site-response effect. Eng Struct 2003; 25(10): 1301-1310.

[35] Berg GV, Housner GW. Integrated velocity and displacement of strong earthquake ground motion. B Seismol Soc Am 1961; 51(2): 175-189.

[36] Desceliers C, Soize C, Cambier S. Non-parametric-parametric model for random uncertainties in non-linear structural dynamics: Application to earthquake engineering. Earthq Eng Struct Dyn 2004; 33(3): 315-327.